Unimolecular Rectification and Other Properties of Monolayers of $CH_3C(O)S\text{-}C_{14}H_{28}Q^+\text{-}3CNQ^-$ and $CH_3C(O)S\text{-}C_{16}H_{32}Q^+\text{-}3CNQ^-$ Organized by Self-Assembly, Langmuir-Blodgett, and Langmuir-Schaefer Techniques[-]

Archana Jaiswal§, Desikan Rajagopal@, M. V. Lakshmikantham‡, Michael P. Cava, and Robert M. Metzger*
Laboratory for Molecular Electronics
Department of Chemistry
University of Alabama
Box 870336
Tuscaloosa, AL 35487-0336, USA

SUPPLEMENTARY MATERIAL

§ Current address: Q-Sense, 808 Landmark Drv., Suite #124, Glen Burnie, MD 21061, USA, email=archanajaiswal1@yahoo.com
@ Current address: Department of Chemistry, University of Washington, Seattle, WA 98195, USA, email= desikanrajagopal@yahoo.com
* Corresponding author; email=rmetzger@bama.ua.edu
‡ Deceased 20 Jan 2006

Synthesis

Compounds **3** ("C14") and **4** ("C16") were synthesized by a different method than that reported for the synthesis of **2** ("C11") [10]. The scheme is outlined in **Figure A**. Several other compounds in the series were also made, with C3, C4, C6, and C8 alkane sections, in place of the C14 and C16 studied in detail here; for completeness, the synthesis of the C3 compound is also given below.

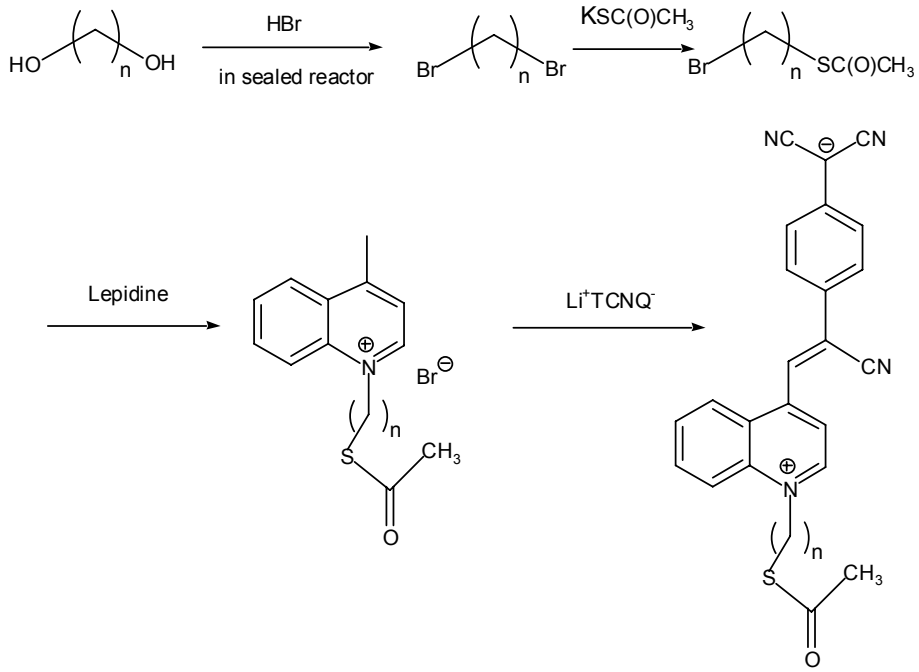

Figure A. Scheme for the syntheses of compounds **3** (n=14) and **4** (n = 16).

1, 14-Tetradecyldibromide

In a sealed high-pressure reactor immersed in an oil bath at 140–150˚C, 1,14-hexadecyldiol (1 g) was reacted with HBr (48% aq. solution) 7-8 hours. The reactor was cooled to room temperature, and opened slowly and carefully. The crude dibromide was obtained in 98% yield as a pale-brown solid, which was filtered and dried. mp 49-52˚C. This crude dibromide was used for further steps without further purification. ^{1}H NMR ($CDCl_3$): δ 3.40 (t, 2H, J = 6 Hz), 1.84 (m, 2H), 1.41 (m, 2H), 1.26 (m, 10H).

14-Thioacetyl-tetradecyl-1-bromide

The reaction was carried out in dilute condition using DMF. 1,14-Tetradecyldibromide (0.5 g, 0.0014 mol) was dissolved in 300 mL commercial DMF in a three necked 500 mL round-bottomed flask, heated on an oil bath at 100-115'C under N_2. Potassium thioacetate (0.090g, 0.00078 mole) was added gradually, over a 3 to 4 h period. The reaction was heated for 4 more hours. The completion of the reaction was monitored by checking aliquots on a TLC plate at regular intervals. The reaction mixture was worked up by evaporating DMF under reduced pressure using a rotary evaporator. The crude product was dissolved in a minimum amount of CH_2Cl_2 and filtered to remove any inorganic salt. The excess CH_2Cl_2 was evaporated, and the crude product was extracted on a Chromatotron using a 2% ethyl acetate : hexane eluent. The product was obtained as a pale-yellow viscous liquid in 45-47% yield. ^{1}H NMR ($CDCl_3$): δ 3.40 (t, 2H), 2.85 (2H), 2.31 (s, 3H), 1. 84 (m, 3), 1.25 (m, 25H).

1 –Tetradecylthioacetyl-lepidinium bromide

A mixture of lepidine (2 g) and thioacetyltetradecylbromide (1 g) was heated on an oil bath at 140˚C for 5 h. The mixture was cooled to room temperature, and the residue was triturated with anhydrous diethyl ether, 3 × 50 mL. The resulting blue viscous quinolinium salt (60%) was dried under vacuum, and was used without further purification.

(Z)-α-Cyano-β-[N-tetradecylthioacetylquinolin-4-ylium)-4-styry1di-cyanomethanide, 3, "C14"

A solution of 1-tetradecylthioacetyllepidinium bromide (0.12 g), pyridine (0.40 g), Li^+TCNQ^- (0.105 g) and DMSO (4 mL) was heated on a steam bath for 3 h. The solution was cooled to room temperature, 10 mL CH_3CN were added, and the solid was filtered, washed with CH_3CN, and air-dried, to yield the expected product **3** in 48% yield as a greenish-blue solid, mp 248˚C (decomp). ^1H NMR (DMSO-d_6): δ 9.43 (d, 1H), 8.74 (d, 1H), 8.55 (d, 1H), 8.48 (d, 1H), 8.44 (s, 1H), 8.25 (t, 1H), 8.02 (t, IH), 7.74 (d, 2H), 6.89 (d, 2H), 4.95 (t, 2H), 2.81 (t, 2H), 2.30 (s, 3H), 1.97(m, 2H), 1.27(m, 24H). Anal. Calcd for $C_{37}H_{42}N_4OS$: C, 75.22; H, 6.91; N, 9.48; S, 5.43. Found: C, 74.88; H, 7.04; N, 9.26

1,16-Hexadecyldibromide

In a sealed reactor immersed in an oil bath maintained at 140-150˚C 1,16-hexadecyldiol (1 g) was reacted with HBr (48% aq solution) for 7-8 h. The reactor was cooled to room temperature, and opened carefully. The crude dibromide, obtained in 98% yield as a pale-brown solid, was filtered and dried, mp: 52-54˚C. This crude dibromide was used without further purification. ^1H NMR ($CDCl_3$): δ 3.35 (t, 2H, J = 6 Hz), 1.85 (m, 2H), 1.57 (m, 2H), 1.26 (m, 10H).

16-Thioacetyl-hexadecyl-1-bromide

The dibromide (0.5 g, 0.0013 mol) was taken in 300 mL of commercial DMF in a three-necked 500 mL round-bottomed flask, which was heated in an oil bath at 100-110˚C under N_2. Potassium thioacetate (0.075 g, 0.00065 mol) was added gradually over 3-4 h. The reaction was further heated for 4 h. The reaction was monitored by TLC at regular intervals. The reaction mixture was worked up by evaporating DMF under reduced pressure using a rotary evaporator. The crude product was dissolved in a minimum amount of CH_2Cl_2, and filtered to remove any inorganic salt. The excess CH_2Cl_2 was evaporated, and the crude product was purified in a Chromatotron, using a 2% ethyl acetate : hexane eluent. The product was obtained as a pale-yellow viscous liquid in 40-42 % yield. ^1H NMR ($CDCl_3$): δ 3.40 (t, 2H), 2.86 (2H), 2.32 (s, 3H), 1.85 (m, 3H), 1.25 (m, 25H).

1-Hexadecylthioacetyl-lepidinium bromide

A mixture of lepidine (2 g) and 16-thioacety1hexadecyl-1-bromide (1 g) was heated on an oil bath at 140˚C for 5 h. The mixture was cooled to room temperature, and the residue was triturated with anhydrous diethyl ether 3 × 50 mL. The resulting blue-colored viscous quinolinium salt (60% yield) was dried under vacuum, and was used without further purification.

(Z)-α-Cyano-β-[N-hexadecylthioacetylquinolin-4-ylium)-4-styry1di-cyanomethanide, 4, "C16"

A solution of 1-hexadecylthioacetyllepidinium bromide (0.18 g), pyridine (0.33 g), Li^+TCNQ^+ (0. 146 g), and DMSO (4 mL) was heated on a steam bath for 3 h. The solution was cooled to room temperature, 10 mL CH_3CN were added, and the solid was filtered, washed with CH_3CN and air-dried, to give expected product **4** in 48% yield as a greenish-blue solid, mp 235–241˚C (decomp). ^1H NMR (DMSO-d_6): δ 9.425 (d, 1H), 8.75 (d, 1H),

8.56 (d, 1H), 8.48 (d, 1H), 8.44 (s, 1H), 8.25 (t, 1H), 8.03 (t, 1H), 7.75 (d, 2H), 6.89 (d, 2H), 4.97 (t, 2H), 2.80 (t, 2H), 2.30 (s, 3H), 1.97 (m, 2H), 1.28 (m, 28H). Anal. Calcd for $C_{39}H_{46}N_4OS$: C, 75.69; H, 7.49; N, 9.05; S, 5.18. Found: C, 75.14; H, 7.33; N, 8.97; S, 4.38.

3-Thioacetyl-n-propane bromide

1,3-propane dibromide (4.0 g) was dissolved in 400 mL commercial DMF in a three necked 500 mL round-bottomed flask, which was heated in an oil bath at 100-110˚C under N_2. Potassium thioacetate (1.2 g, 0.0196 mol) was added gradually over 32 h. The reaction was further heated for 4 h. The reaction was monitored by TLC at regular intervals. The reaction mixture was worked up by evaporating DMF under reduced pressure using a rotary evaporator. The crude product was dissolved in a minimum amount of CH_2Cl_2 and filtered, to remove any inorganic salt. The excess CH_2Cl_2 was evaporated, and the crude product was purified in a Chromatotron, using a 4% ethyl acetate : hexane eluent. The product was obtained as a pale-yellow viscous liquid in 52-54 % yield. ^{1}H NMR ($CDCl_3$): δ 3.41 (t, 2H), 2.82 (2H), 2.32 (s, 3H), 1.81 (m, 2H).

1-Propylthioacetyllepidinium bromide

A mixture of lepidine (2 g) and thioacetylpropanebromide (1 g) was heated on an oil bath at 140˚C for 5 h. The mixture was cooled to room temperature, and the residue was triturated with anhydrous diethyl ether 3 × 50 mL. The resulting blue-colored viscous quinolinium-salt (57 %) was dried under vacuum, and was used without further purification.

(Z)-α-Cyano-β-[N-propylthioacetylquinolin-4-ylium)-4-styry1di-cyanomethanide

A solution of 1-propane thioacetyllepidinium bromide (0.260 g), pyridine (0.33 g), Li^+TCNQ^- (0.326 g) and DMSO (4 mL) was heated on a steam bath for 3 h. The solution was cooled to room temperature; 10 mL CH_3CN were added, and the solid was filtered, washed with CH_3CN, and air-dried, to give expected product in 51% yield as a greenish-blue solid, mp 272-273.5˚C (decomp). ^{1}H NMR (DMSO-d_6): δ 9.37 (d, 1H), 8.70 (d, 1H), 8.49 (d, 1H), 8.48 (d, 1H), 8.44 (s, 1H), 8.25 (t, 1H), 8.03 (t, 1H), 7.65 (d, 2H), 6.84 (d, 2H), 4.97 (t, 2H), 2.97 (t, 2H), 2.28 (s, 3H), 2.20 (m, 2H). Anal. Calcd for $C_{20}H_{20}N_4OS$: C, 71.54; H, 4.62; N, 12.83; S, 7.34. Found: C, 71.65; H, 4.78; N, 12.54; S, 7.10.

XPS Spectra

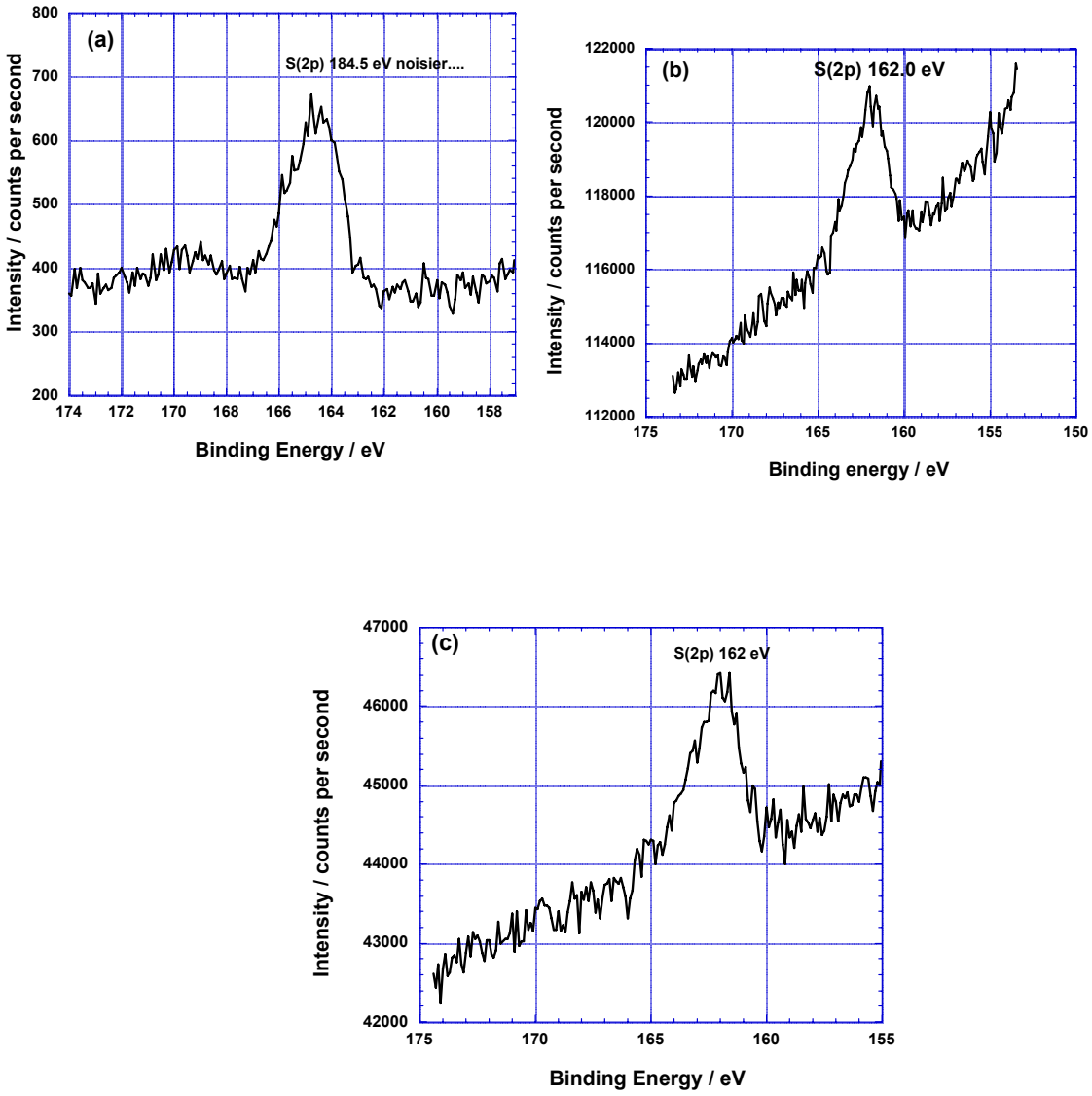

Figure B. High-resolution S(2p) XPS spectra of (a) cast film of $CH_3C(O)SC_{14}H_{28}Q^+$-3CNQ$^-$, **3**, on HOPG (b) SAM of $CH_3C(O)SC_{14}H_{28}Q^+$-3CNQ$^-$,**3**, on Au (c) SAM of $CH_3C(O)SC_{16}H_{32}Q^+$-3CNQ$^-$, **4**, on Au.

Angle-resolved X-ray photoelectron spectroscopy (XPS): Molecular orientation

Table A. Ratio of integrated S(2p) and N(1s) XPS peak areas of monolayers (SAM, LS, LB up-stroke, and LB down-stroke) of $CH_3C(O)SC_{14}H_{28}Q^+$-3CNQ$^-$, **3**, and $CH_3C(O)SC_{16}H_{32}Q^+$-3CNQ$^-$, **4** at different take-off angles (TOA). The entry "Down" or "Up" for S position indicates that the S atom is closest to the Au surface, or closest to the top of the monolayer, respectively. The S(2p)% and N(1s) are given to two significant figures, and are considered reliable to no better than ±5%, while the ratio of the signal intensities (N/S) is considered reliable to ±0.2. The column "N/S trend" indicates with an up-arrow ↑, down-arrow ↓, equal sign =, that, with increasing TOA, the N/S ratio either increases, or decreases, or does not change, respectively. In the last entry, "OK" indicates that the trend confirms the relative position of the S atoms in the film, or agrees with the disorder in a SAM.

Compound	Film type	Fig.	S position	TOA	S(2p)(%)	N(1s) (%)	N/S	N/S trend
3	SAM	C	Down	0°	46	54	1.2	
				15°	46	54	1.2	
				30°	47	53	1.2	
				45°	46	54	1.2	= (OK)
3	LS	D	Down	0°	25	75	3.0	
				15°	20	80	4.0	
				30°	17	83	4.8	
				45°	16	84	5.4	↑ (OK)
3	Down-stroke LB	E	Down	0°	24	76	3.2	
				15°	25	75	3.0	
				30°	23	77	3.4	
				45°	18	82	4.6	↑ (OK)
3	Up-stroke LB	F	Up	0°	14	86	6.4	
				15°	18	82	4.6	
				30°	21	79	3.8	
				45°	26	74	2.8	↓ (OK)
4	LS	G	Down	0°	11	89	8.4	
				15°	10	90	9.0	
				30°	10	90	9.0	
				45°	6	94	15	↑ (OK)
4	Up-Stroke LB	H	Down	0°	4	96	24	
				15°	9	91	10	
				30°	13	89	6.8	↓ (OK)

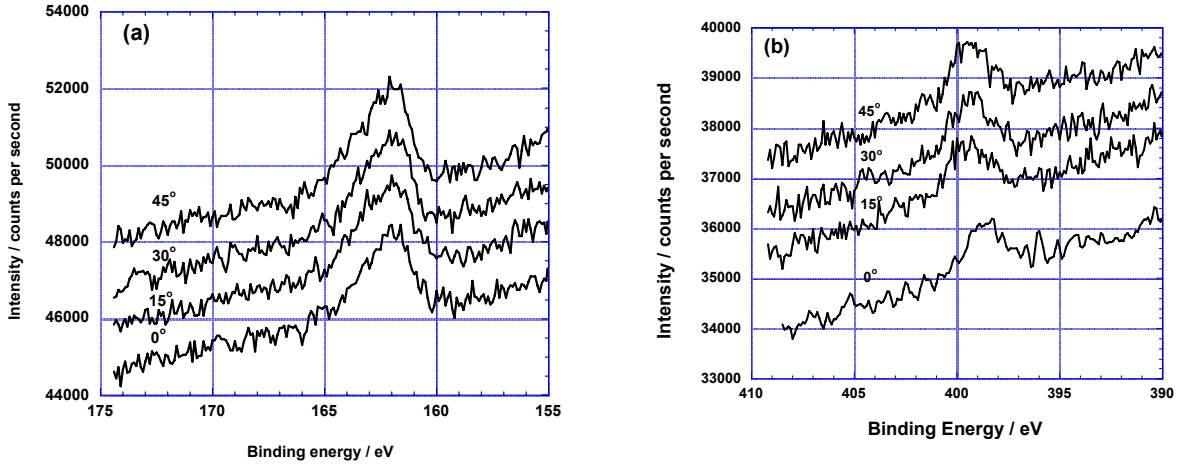

Figure C. High-resolution XPS of SAM of $CH_3C(O)SC_{14}H_{28}Q^+$-3CNQ$^-$, **3** at different TOAs (0˚, 15˚, 30˚, 45˚): (a) S (2p) (b) N(1s). The S and N peak intensities were obtained by integrating the spectra between 161 and 163 eV, and between 396 and 402 eV, respectively.

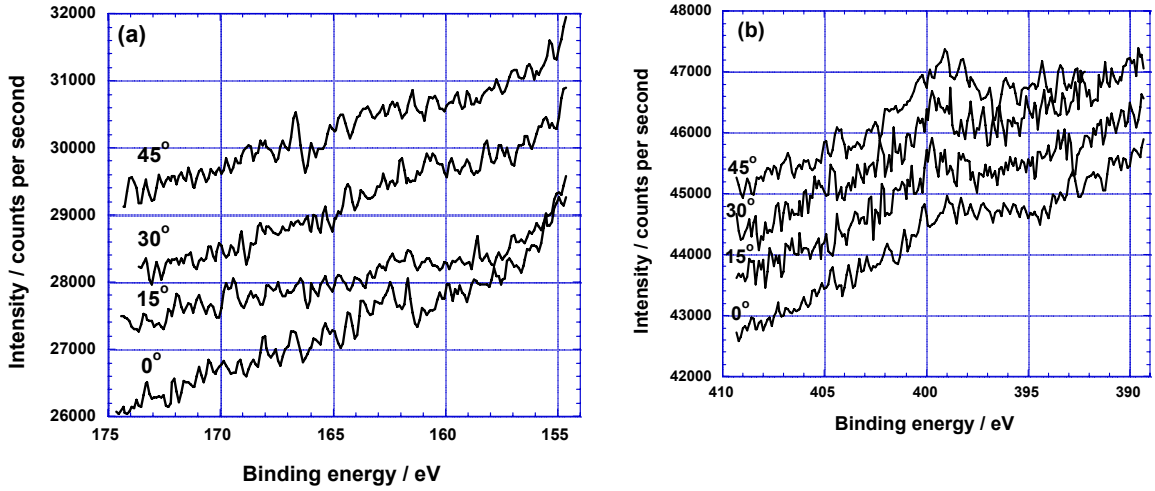

Figure D. High-resolution XPS of LS monolayer of $CH_3C(O)SC_{14}H_{28}Q^+$-3CNQ$^-$, **3** at different TOAs: (a) S(2p) (b) N(1s).

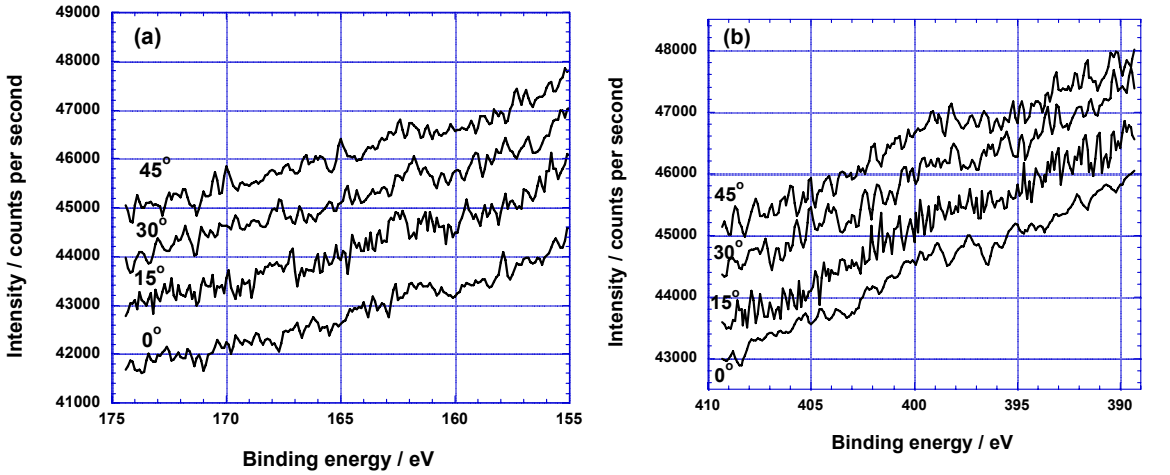

Figure E. High-resolution XPS of LB down-stroke monolayer of $CH_3C(O)SC_{14}H_{28}Q^+$-3CNQ$^-$, **3** at different TOAs: (a) S(2p) (b) N(1s).

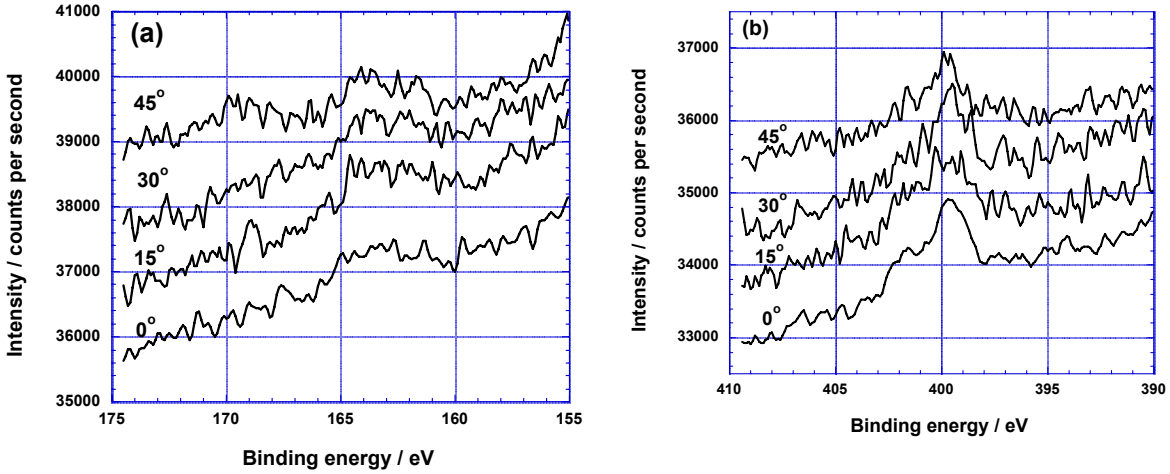

Figure F. High-resolution XPS of LB up-stroke monolayer of $CH_3C(O)SC_{14}H_{28}Q^+$-3CNQ$^-$, **3** at different TOAs: (a) S (2p) (b) N(1s).

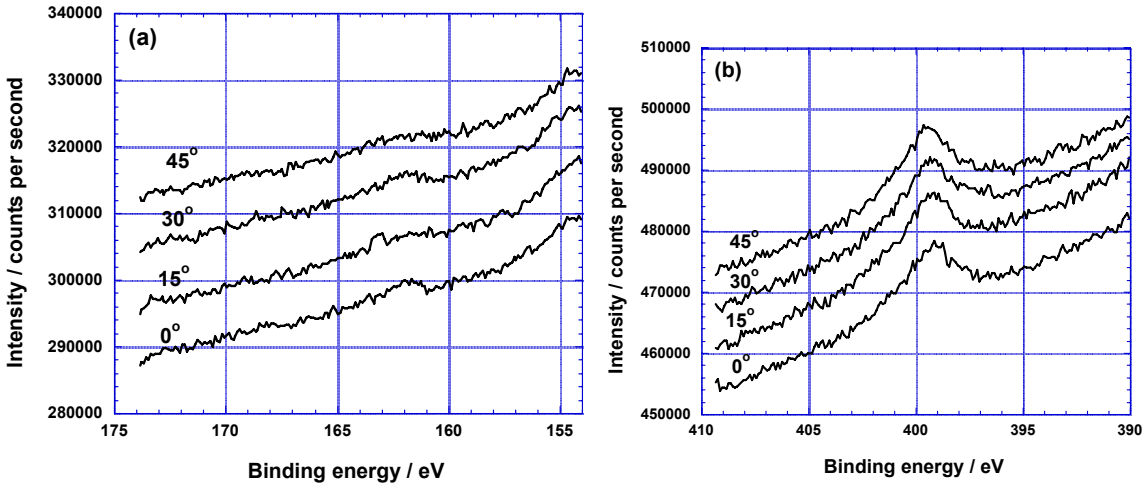

Figure G. High-resolution XPS for LS monolayer of $CH_3C(O)SC_{16}H_{32}Q^+$-$3CNQ^-$, **4** at different TOAs: (a) S(2p) (b) N(1s).

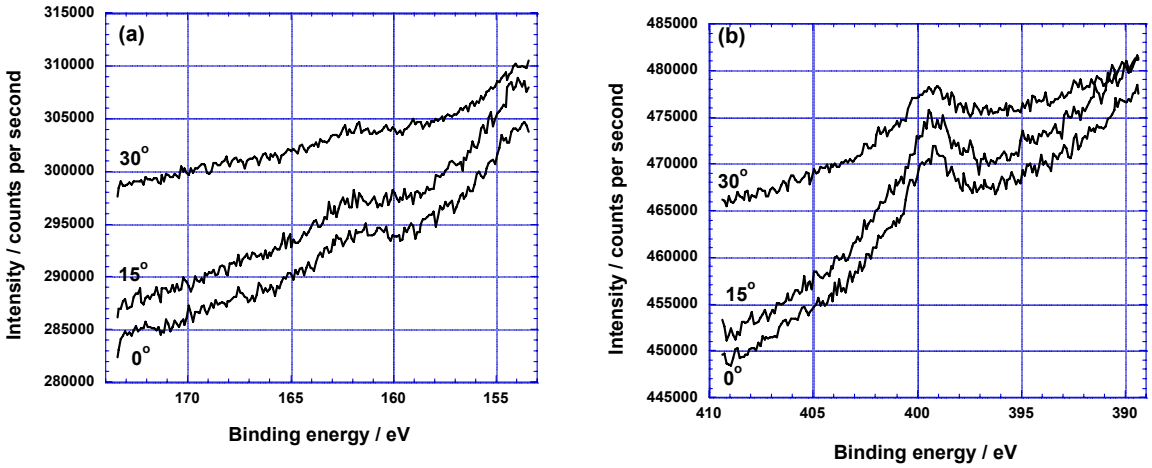

Figure H. High-resolution XPS of LB up-stroke monolayer of $CH_3C(O)SC_{16}H_{32}Q^+$-$3CNQ^-$, **4** at different TOAs: (a) S(2p) (b) N(1s).

Infra-Red Spectrum of KBr Pellet and Reflection-Absorption Infrared Spectroscopy (RAIRS)

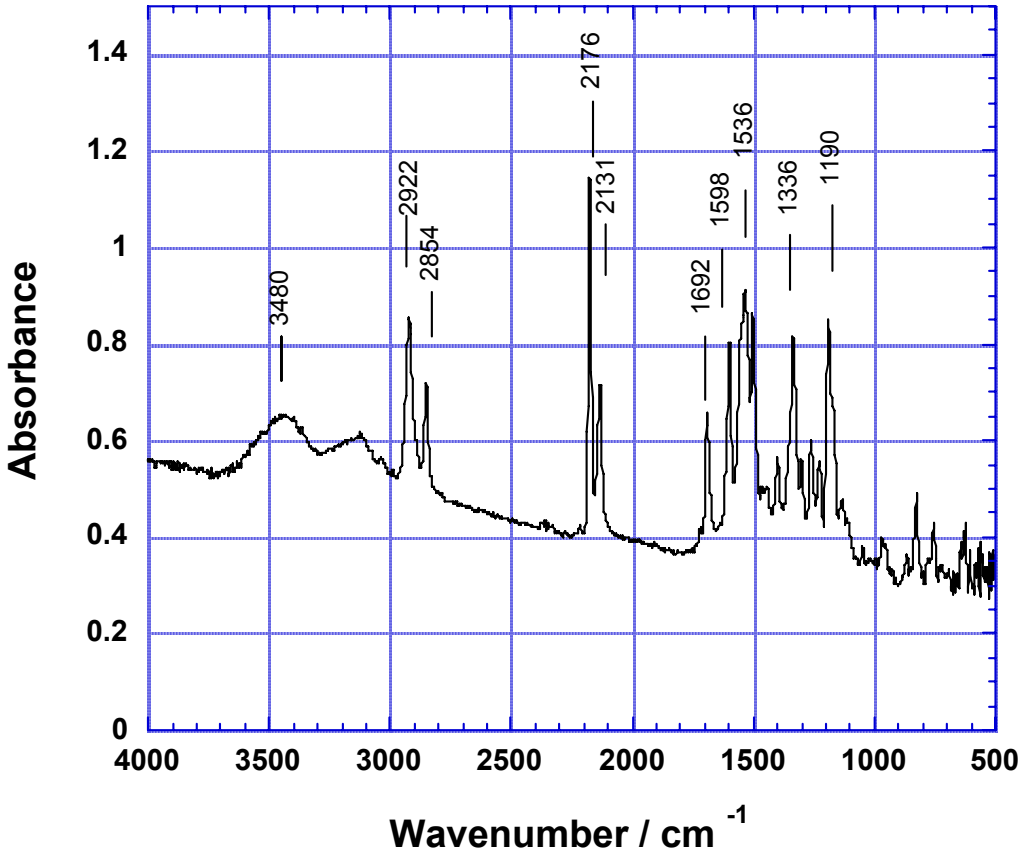

Figure I. (**Same data as Figure 4a**) FTIR spectrum of $CH_3C(O)SC_{14}H_{28}Q^+$-3CNQ$^-$, **3** in solid KBr. (The closely related $CH_3C(O)SC_{16}H_{32}Q^+$-3CNQ$^-$, **4** in solid KBr exhibits the same features, and is not shown here).

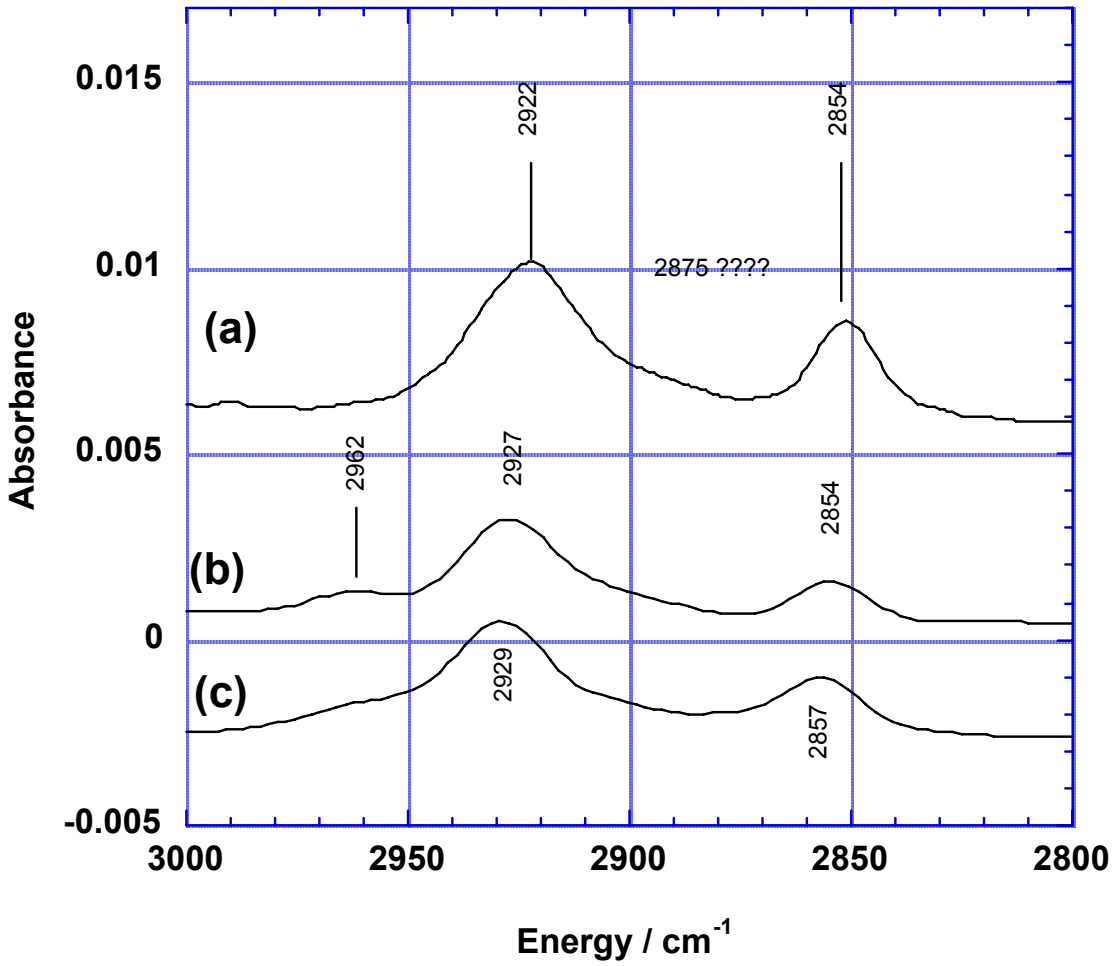

Figure J. Detail of **Figure 4**: (a) FTIR spectrum of **3** in solid KBr. (b) RAIRS spectrum of LB upstroke monolayer of **3**; (c) RAIRS spectrum of LB upstroke monolayer of **4**.

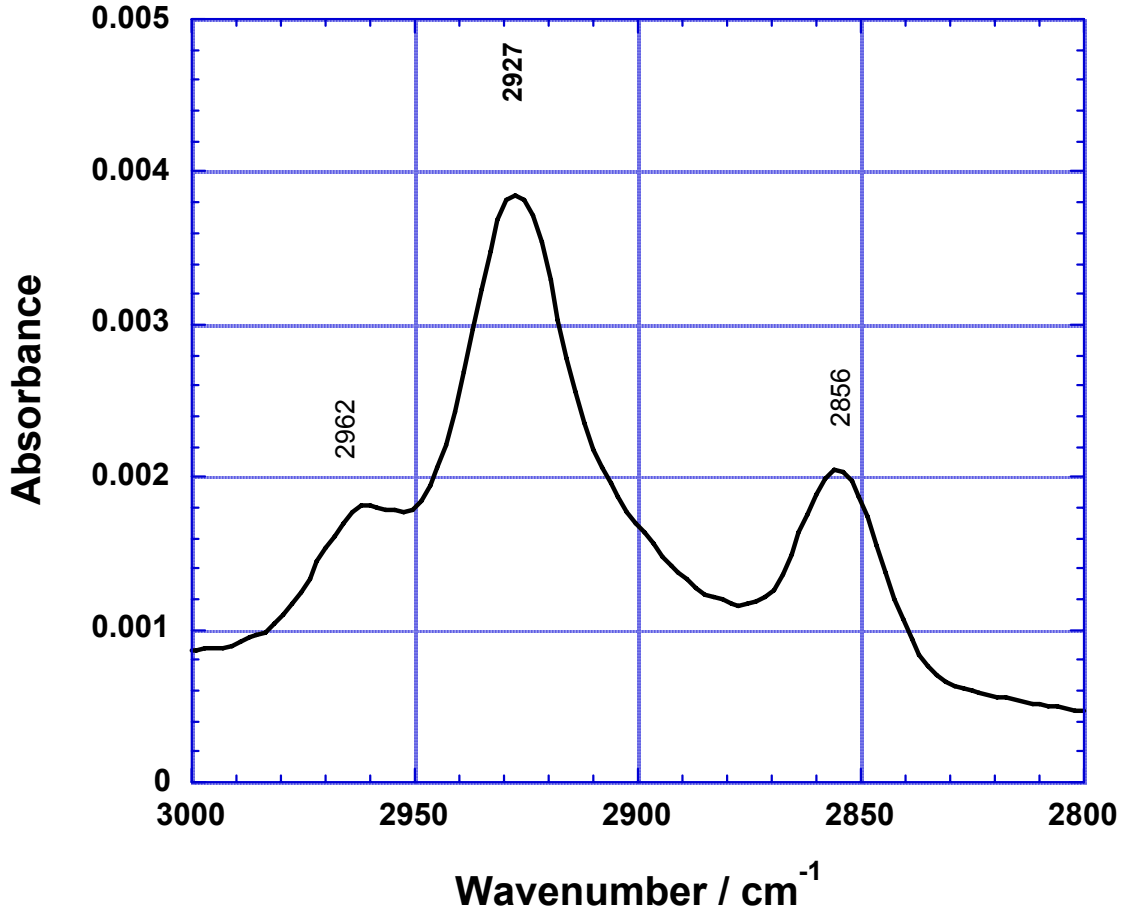

Figure K. Detail of RAIR spectrum of LB down-stroke monolayer of **3.**

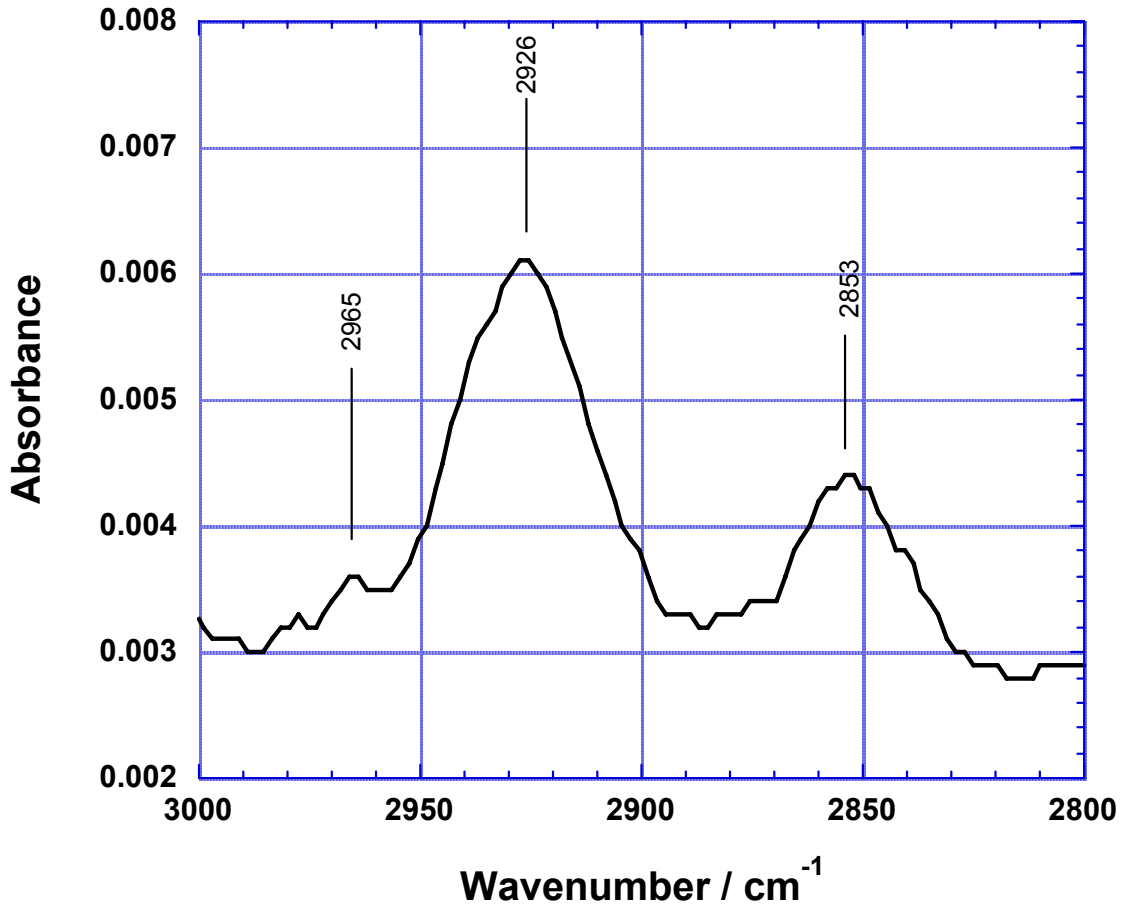

Figure L. RAIR spectrum of LS monolayer of **3**, after 90 degree rotation of sample

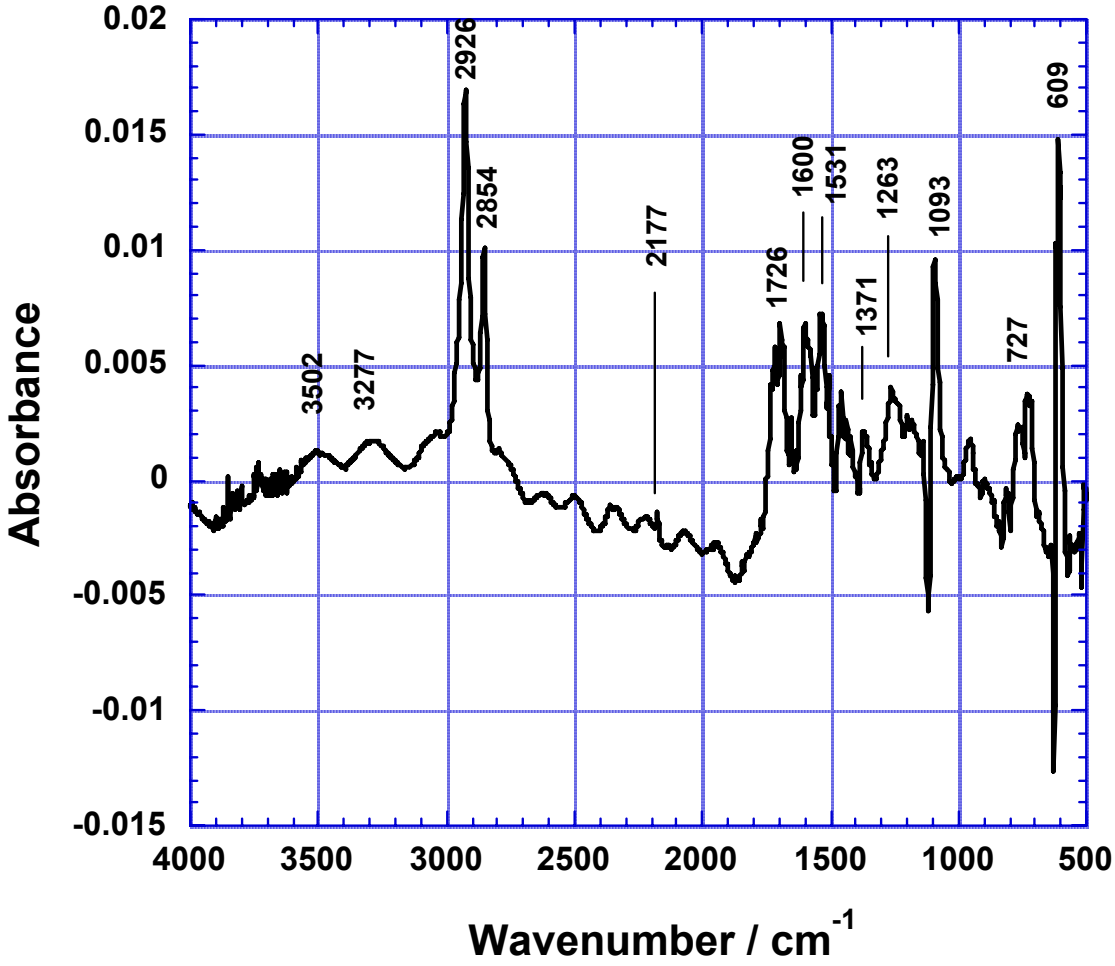

Figure M. RAIR spectrum of 10 LB monolayers of $CH_3C(O)SC_{16}H_{32}Q^+$-$3CNQ^-$, **4** on Au.

RAIRS of the monolayers of compound **3** and **4** have also been recorded after a 90° rotation of the substrates in the plane of the sample, around the substrate normal, in order to learn more about the film organization. At 0˚ rotation, the incoming and outgoing IR beams form a plane, that contains the direction, in which the films were deposited, while at a rotation of 90˚ around the normal to the substrate, the direction of film deposition is at 90˚ from the direction of the incoming and reflected IR beams. This sample rotation interrogates the orientational anisotropy in the plane of the monolayer. The spectra recorded at the two different angles have different peak intensities in all the monolayers, indicating that these films are well-organized; this difference is most prominent in the case of LS monolayer of compound **3** (**Figure L**). The peaks corresponding to the aromatic ring in the region 3100 to 3000 cm^{-1} (CH stretching) 1600 to 1440 cm^{-1} (C=C stretching) 1300 to 1000 cm^{-1} (in-plane CH deformation) and 950 to 550 cm^{-1} (out-of-plane CH deformation) intensify drastically upon a 90˚ rotation of the substrate, while the peaks corresponding to the long alkyl chains at 2927 and 2854 cm^{-1} (-CH_2 asymmetric and symmetric stretching frequencies, respectively) remain constant (see **Figures P and Q**). Thus, the LS monolayer of compound **3** has the most ordered organization among all the monolayer types.

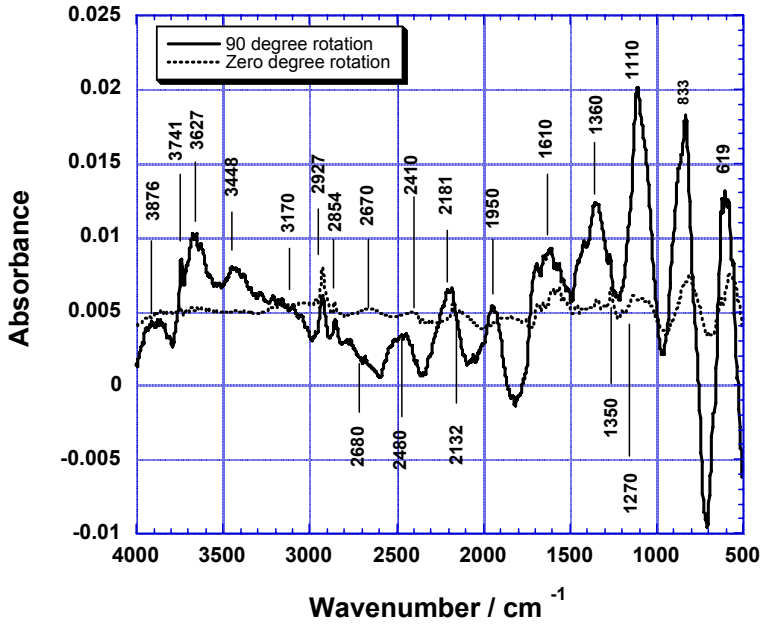

Figure N. RAIR spectra of LS monolayer of $CH_3C(O)SC_{14}H_{28}Q^+$-3CNQ^-, **3** on Au after 0° (dashed line) and 90° (solid line) rotations of the sample about the substrate normal.

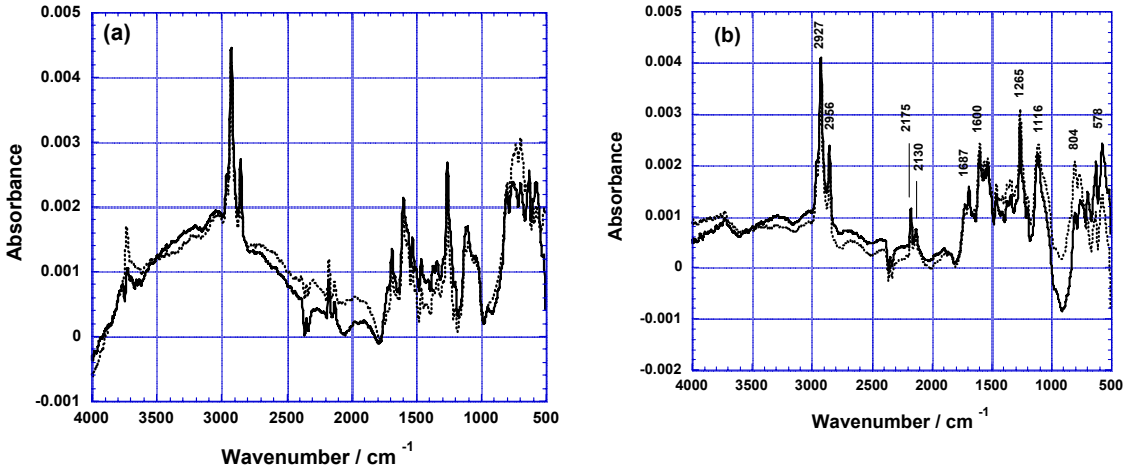

Figure P. RAIR spectra of LB monolayer of $CH_3C(O)SC_{14}H_{28}Q^+$-3CNQ$^-$, **3** on Au: (a) up-stroke (b) down-stroke deposition, after 0° (solid line) and 90° (dashed line) rotations of the sample about the substrate normal.

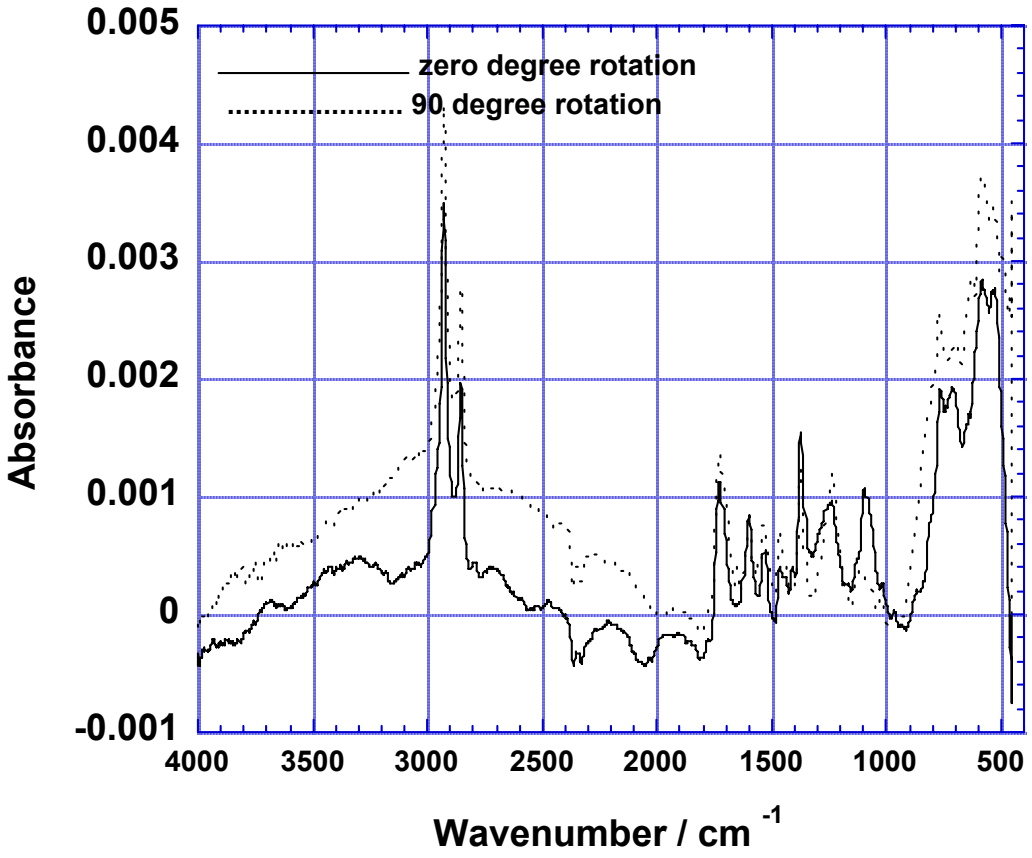

Figure Q. RAIR spectra of LB upstroke monolayer of $CH_3C(O)SC_{16}H_{32}Q^+$-3CNQ$^-$, **4**, on Au after 0° and 90° rotations of the sample about the substrate normal.

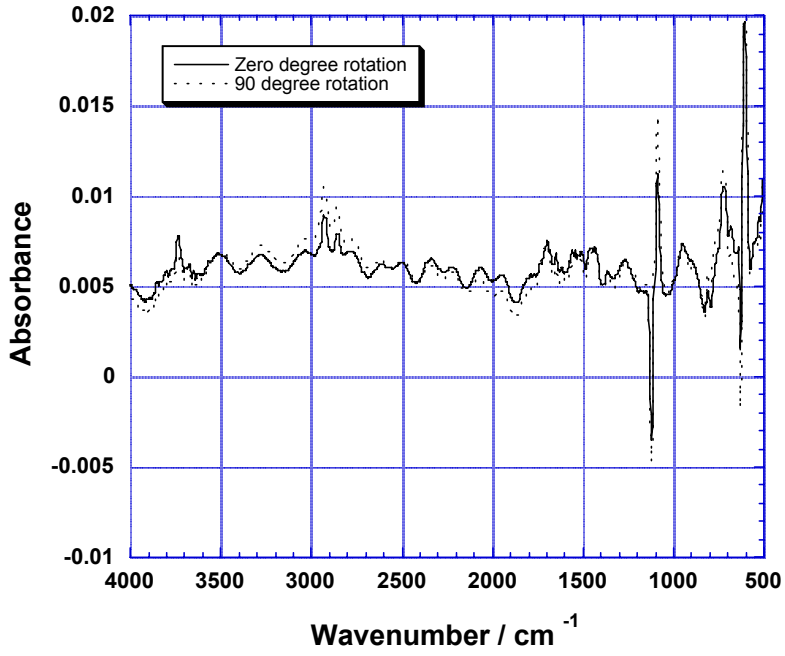

Figure R. RAIR spectra of LS monolayer of $CH_3C(O)SC_{16}H_{32}Q^+$-3CNQ^-, **4** on Au after 0° (solid line) and 90° (dotted line) rotations of the sample about the substrate normal.

Table B. Maximum bias V_{max}, maximum current I_{max} at V_{max} and rectification ratios for various types of monolayers of $CH_3C(O)SC_{14}H_{28}Q^+$-$3CNQ^-$, **3** and $CH_3C(O)SC_{16}H_{32}Q^+$-$3CNQ^-$, **4**. A minus sign (-) was placed before V_{max} if the rectifier has higher current at negative bias, i.e. if the "forward current" for that rectifier is at $V < 0$.

Figure#	Molecule	Film type	V_{max} Volts	I_{max} Ampères	RR
6	**3**	LB up-stroke	0.9	0.00037	4.00
Sa	**3**	LB down-stroke	(-)2.0	0.00565	2.03
Sb	**3**	"	(-)3.0	0.00757	0.96
Sc	**3**	"	(-)3.5	0.0114	1.40
Sd	**3**	"	(-)5.0	0.0209	1.76
Ta	**3**	LS	(-)1.0	0.000309	1.04
Tb	**3**	"	1.5	0.000742	1.16
Tc	**3**	"	2.0	0.00282	1.44
Td	**3**	"	(-)2.5	0.0113	1.46
Te	**3**	"	(-)3.0	0.0289	1.65
Tf = 7a	**3**	"	(-)3.5	0.0552	1.64
Ua	**3**	LS	(-)3.5 initial	0.0502	1.80
			(-)3.5 final	0.0265	2.98
Ub = 7b	**3**	"	(-)4.0	0.0501	2.00
Uc	**3**	"	6.0	0.1000	1.00
Va	**3**	LS	1.0	0.00000255	2.20
Vb	**3**	"	1.5	0.000182	6.96
Vc	**3**	"	2.0	0.00109	2.79
Vd	**3**	"	2.5	0.00349	1.44
Ve	**3**	"	3.0	0.0081	1.00
Vf	**3**	"	(-)3.5	0.0167	1.16
Vg	**3**	"	(-)4.0	0.0285	1.33
Vh = 8	**3**	"	(-)4.5	0.0409	1.52
Wa	**3**	"	(-)5.0	0.0575	1.54
Wb	**3**	"	(-)6.0	0.0947	1.05
Xa	**4**	LB up-stroke	1.5	0.00000232	7.14
Xb = 9	**4**	"	2.0	0.0000202	7.42
Xc	**4**	"	2.5	0.0000847	1.60
Xd	**4**	"	3.0	0.000289	1.30
Xe	**4**	"	(-)3.5	0.000784	1.49
Ya	**4**	LB up-stroke	1.1	2.70 E-09	56.8
Yb	**4**	"	1.2	1.35 E-08	622
Yc = 10	**4**	"	1.3	2.96 E-08	57.2
Za	**4**	LS	(-)1.0	4.12 E-06	1.16
Zb	**4**	"	(-)1.5	0.0000103	3.83
Zc	**4**	"	(-)2.0	0.0000311	3.99
Zd	**4**	"	(-)3.0	0.000178	2.75
Ze	**4**	"	(-)4.0	0.0000827	6.18
Zf	**4**	"	(-)6.0	0.000138	13.5
Zg	**4**	"	(-)10.0	0.000170	46.1

Zh = 11 **4** “ (-)12.0 0.000191 47.6

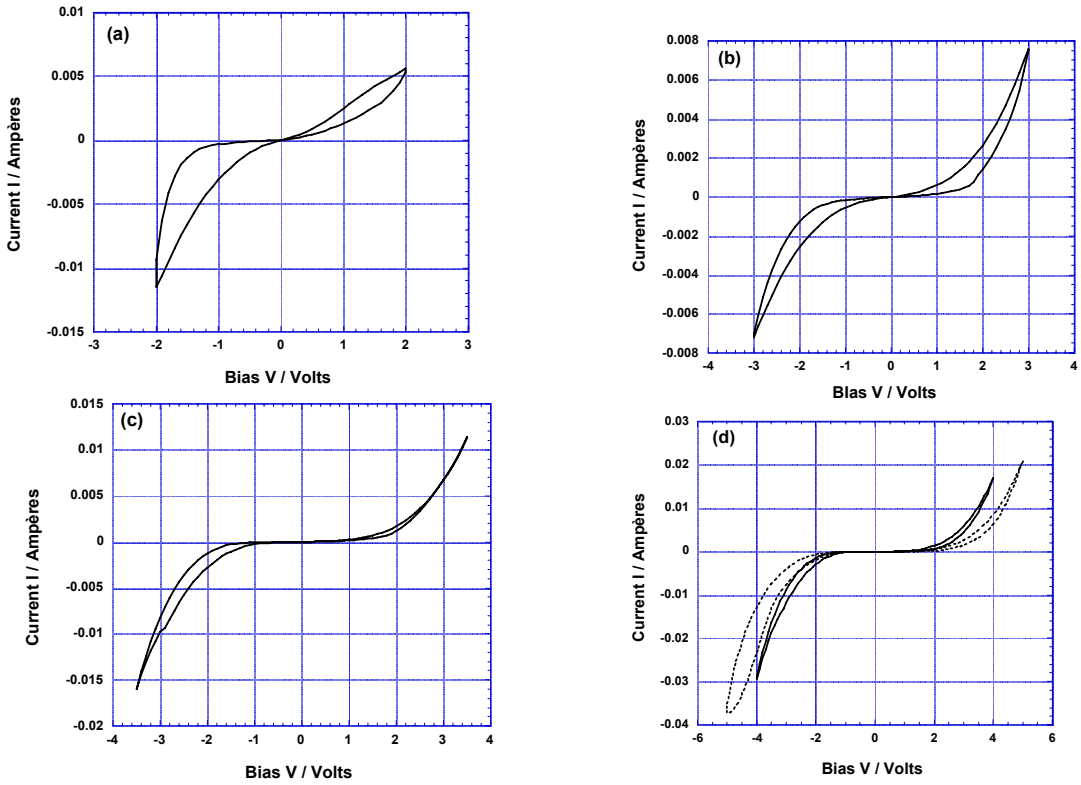

Figure S. I-V evolution of a single down-stroke LB monolayer of $CH_3C(O)SC_{14}H_{28}Q^+$-3CNQ$^-$, **3** sandwiched between two Au electrodes: the device rectifies at V < 0: (a) RR = 5.27 at – 2.0 Volts; (b) RR = 0.961 at – 3.0 Volts; (c) RR = 1.40 at -3.5 Volts; (d) RR = 1.74 at –4.0 Volts (first cycle: solid line); RR = 1.76 at – 5.0 Volts (second cycle: dotted line).

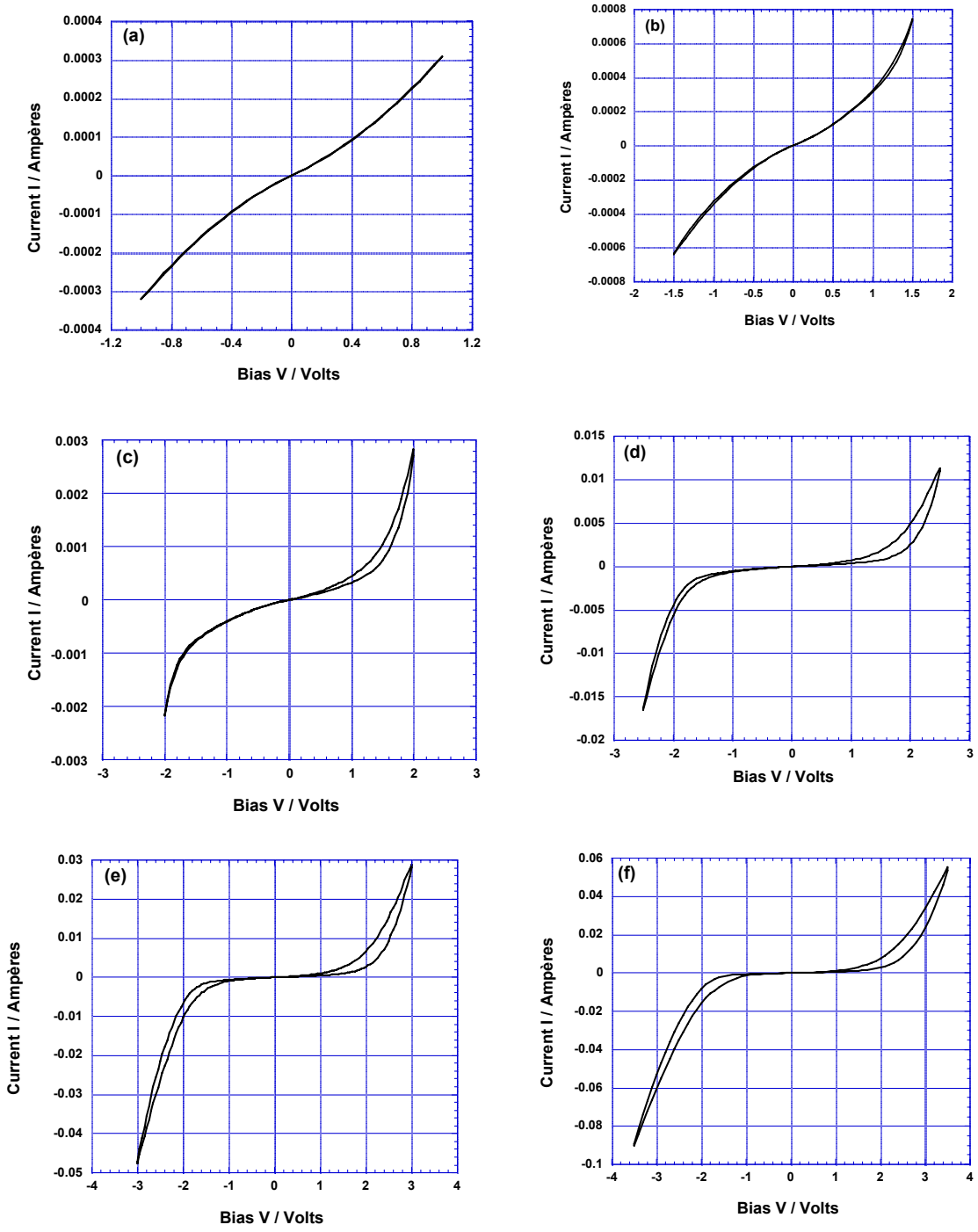

Figure T. I-V evolution of a single LS monolayer of $CH_3C(O)SC_{14}H_{28}Q^+$-$3CNQ^-$, **3** sandwiched between two gold electrodes, and measured repeatedly (pad1): the pad at first rectifies, barely, at V < 0, then rectifies at V > 0, then finally settles down to rectify at V < 0: (a) RR = 1.04 at –1.0 Volts; (b) RR=1.16 at +1.5 Volts (c) RR=1.44 at +2.0 Volts; (d) RR=1.46 at –2.5 Volts; (e) RR = 1.65 at –3.0 Volts; (f) RR= 1.64 at –3.5 Volts (**Figure Td** is the same as **Figure 7a**).

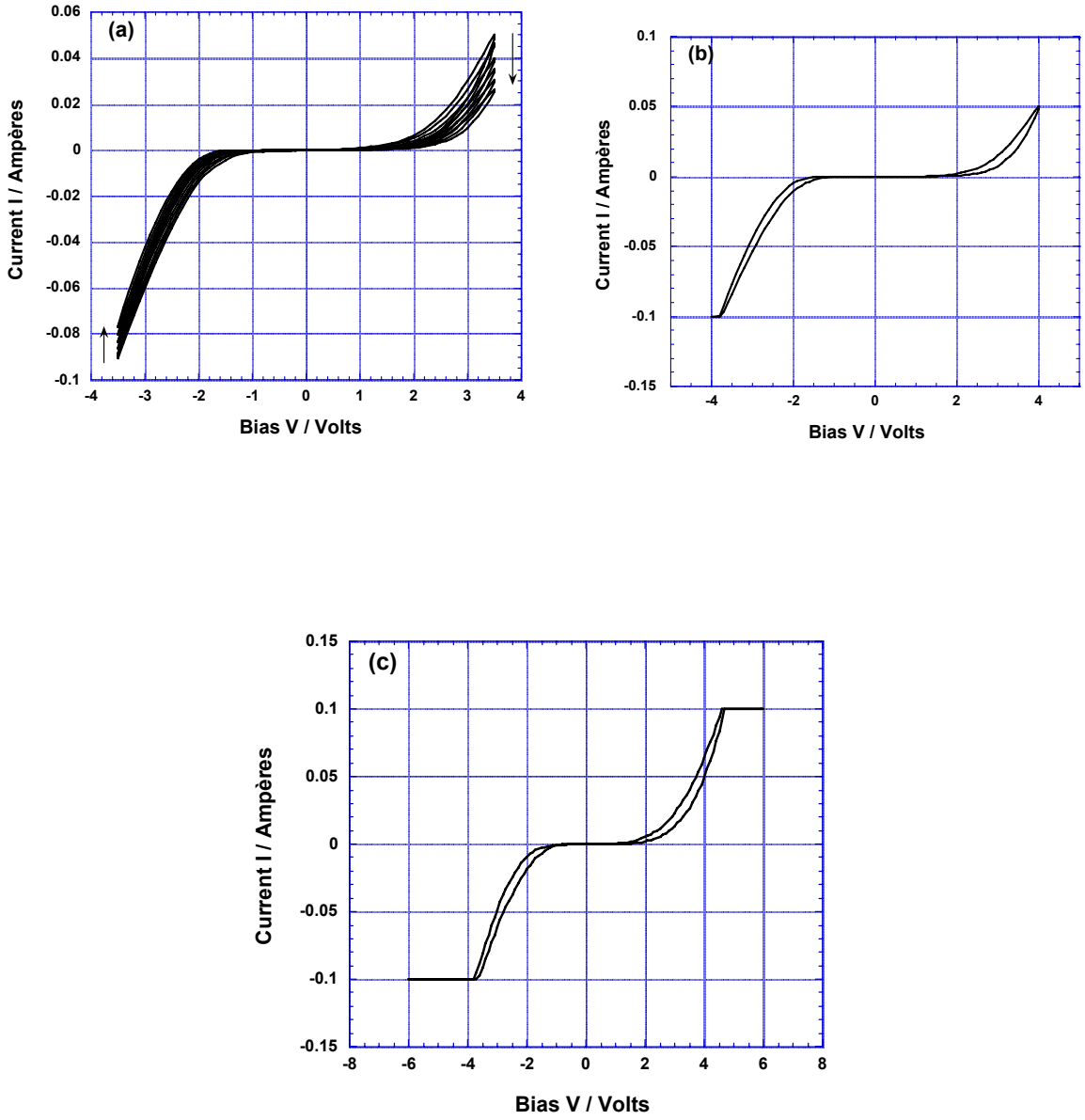

Figure U. Evolution of I-V plot for an LS monolayer of $CH_3C(O)SC_{14}H_{28}Q^+$-3CNQ^-, **3** sandwiched between two Au electrodes (pad 1 continued: same pad as in Figure 27). (a) RR= 1.80 (initially) at -3.5 Volts, with currents decreasing in magnitude, at both positive and negative bias in the direction shown by the two arrows, until RR= 2.98 after 6 cycles; (b) RR= 2.00 at –4.0 Volts; close to -4.0 Volts, the measuring circuit limit of –0.1 Ampères has been reached; (c) measuring further, beyond ±4.5 Volts, the device stops rectifying, does not short out, but reaches the maximum current limits (positive or negative) allowed by the measuring electronics. (**Figure Ub is the same as Figure 7b**)

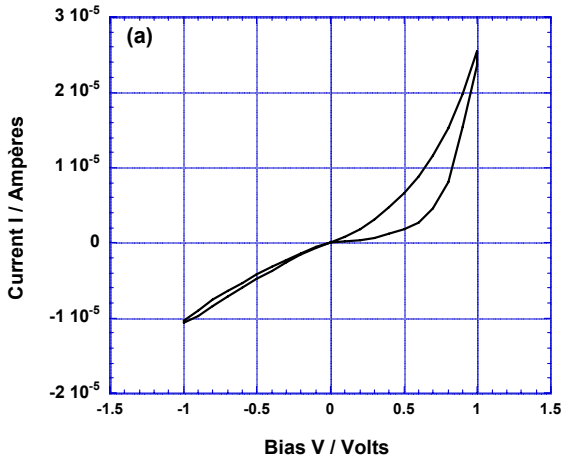

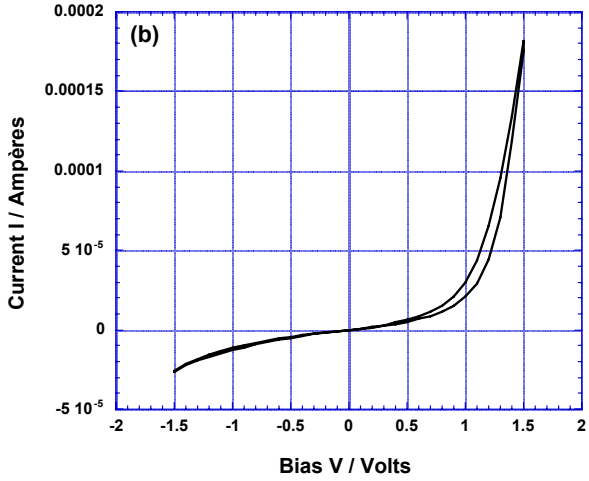

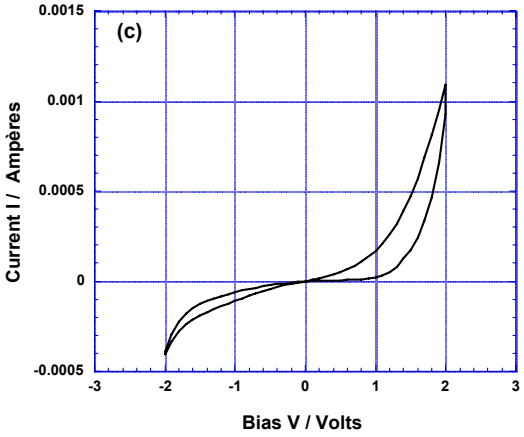

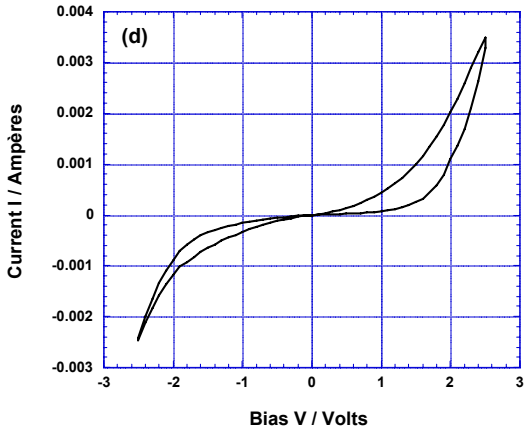

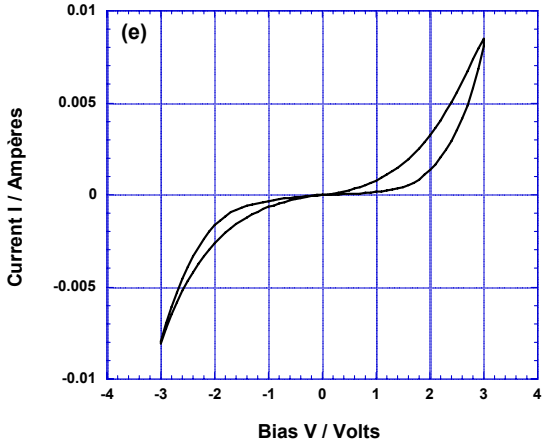

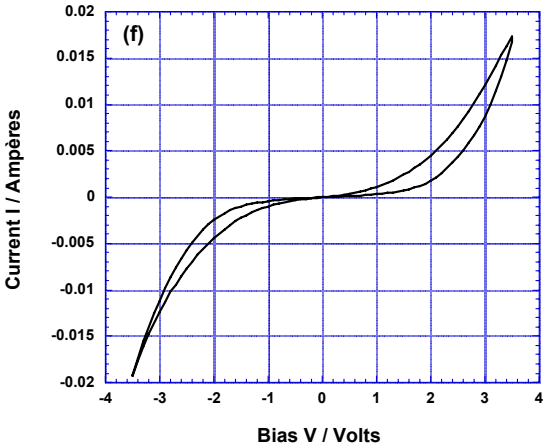

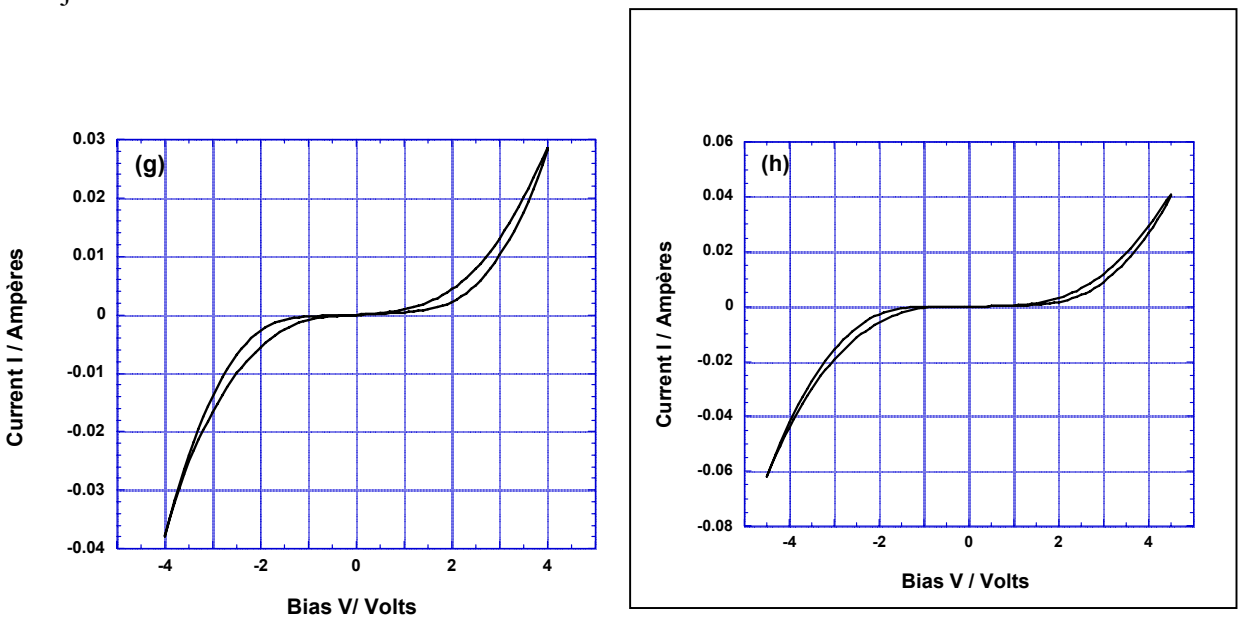

Figure V. I-V behavior of LS monolayer of $CH_3C(O)SC_{14}H_{28}Q^+$-3CNQ$^-$, **3** sandwiched between two Au electrodes (pad2). (a) RR= 2.20 at 1.0 Volt; (b) RR = 6.96 at 1.5 Volt; (c) RR=2.79 at 2.0 Volt; (d) RR = 1.44 at 2.5 Volt; (e) RR = 1.00 at 3.0 Volt; (f) RR=1.16 at – 3.5 Volt; (g) RR = 1.33 at –4.0 Volt; (h) RR = 1.52 at – 4.5 Volt. (**Figure Vh** is the same as **Figure 8**)

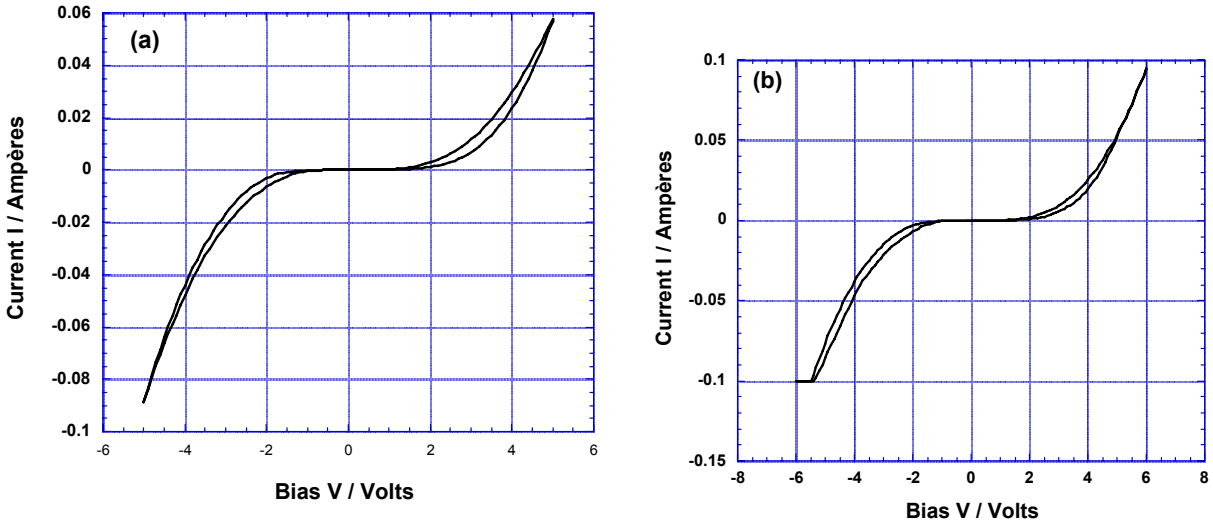

Figure W. I-V behavior of LS monolayer of $CH_3C(O)SC_{14}H_{28}Q^+$-3CNQ$^-$, **3** sandwiched between two Au electrodes (same Pad as in Figure V (pad2 continued). (a) RR = 1.54 at –5.0 Volt; (b) RR = 1.05 at –6.0 Volts (measurement saturates)

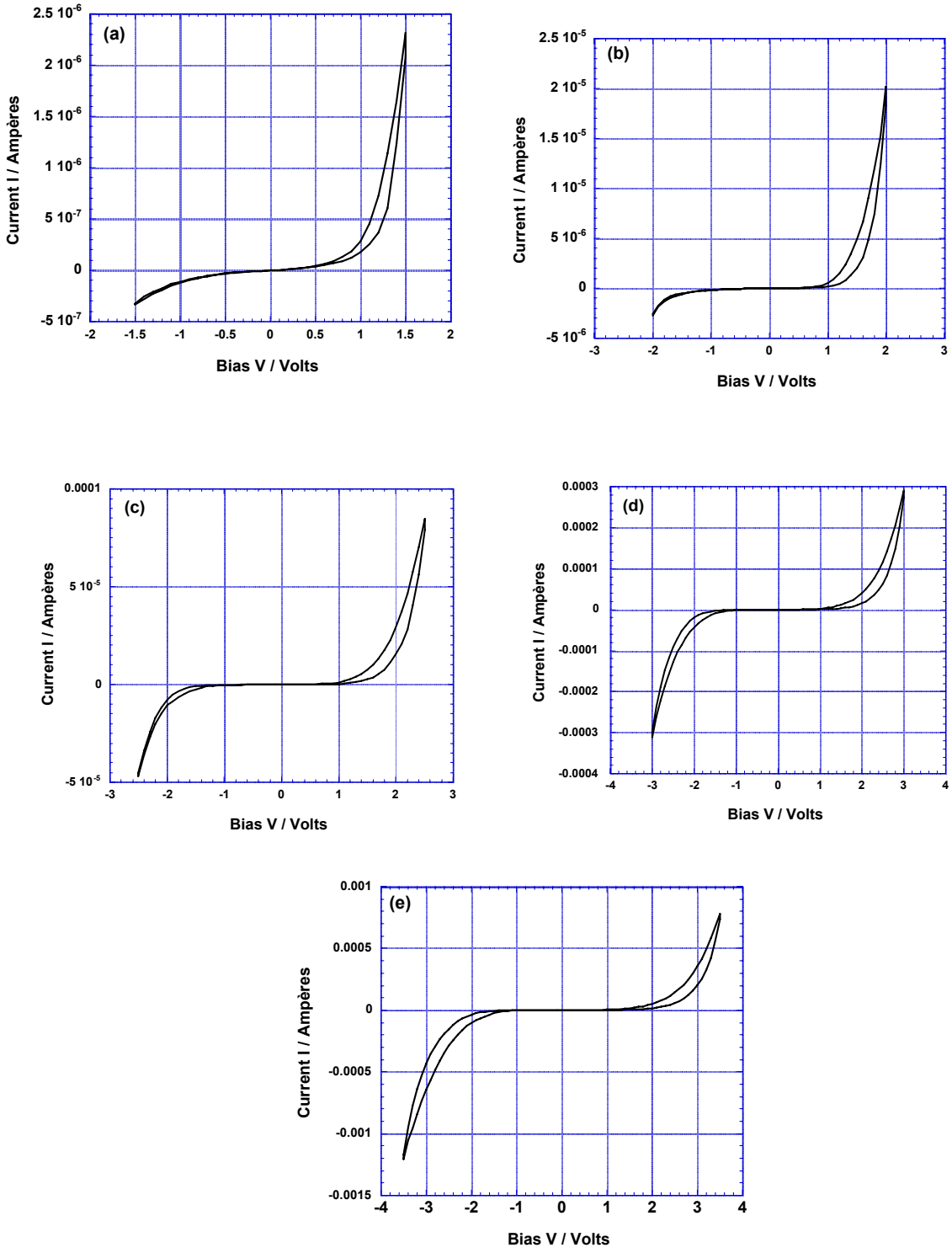

Figure X. I-V behavior of up-stroke LB monolayer of $CH_3C(O)SC_{16}H_{32}Q^+$-3CNQ$^-$, **4** sandwiched between two Au electrodes (pad 1): (a) RR = 7.14 at 1.5 Volt; (b)

RR = 7.42 at 2.0 Volts; (c) RR = 1.60 at 2.5 Volts; (d) RR = 1.30 at 3.0 Volts; (e) RR = 1.49 at –3.5 Volts. **(Figure Xb** is the same as **Figure 9).**

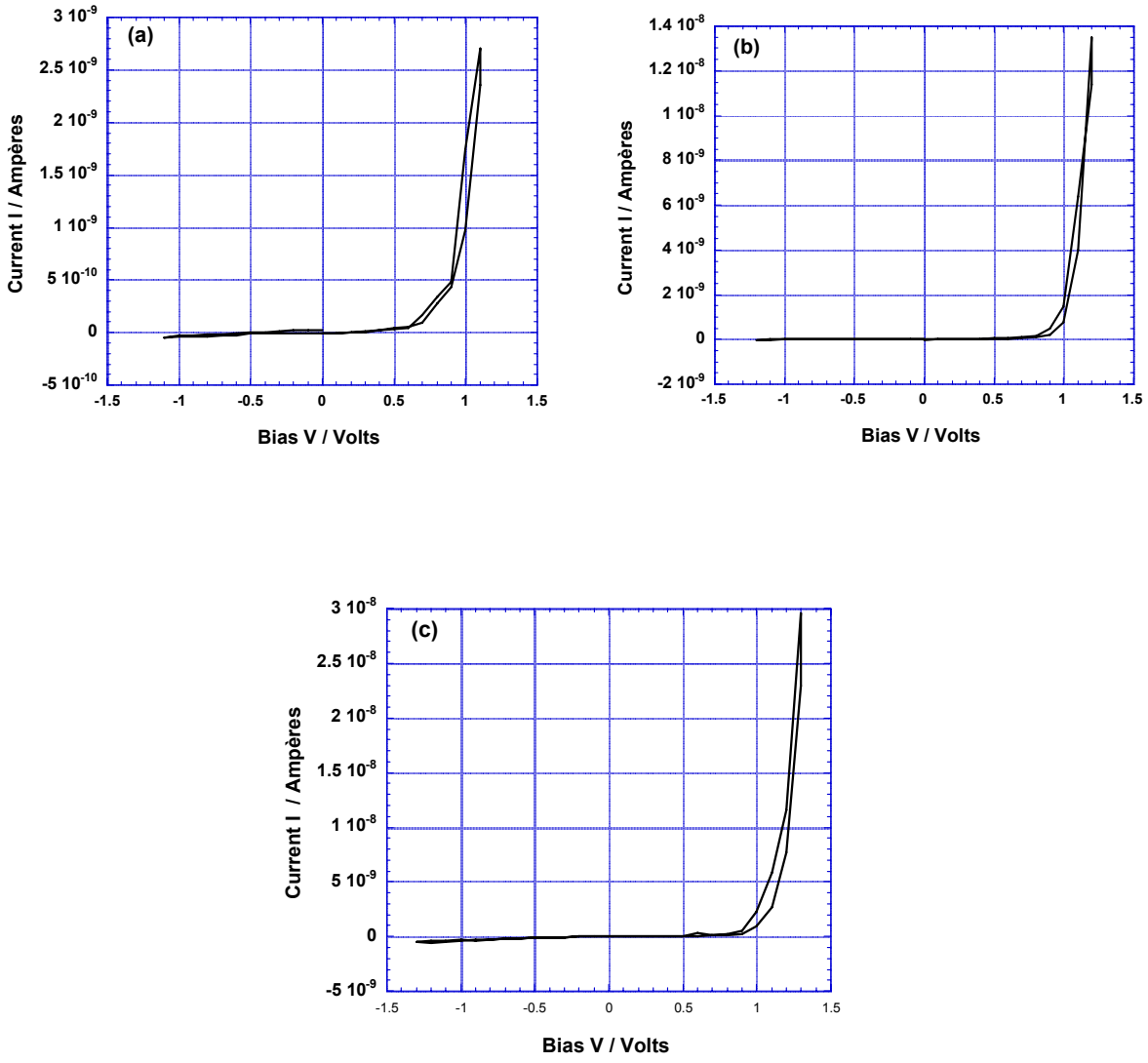

Figure Y. I-V behavior of up-stroke LB monolayer of $CH_3C(O)SC_{16}H_{32}Q^+$-3CNQ$^-$, **4** sandwiched between two Au electrodes (pad 2). (a) RR = 56.8 at 1.1 Volt; (b) RR= 622 at V = 1.2 Volts; (c) RR = 57.2 at 1.3 Volts (**Figure Yc** is the same as **Figure 10**).

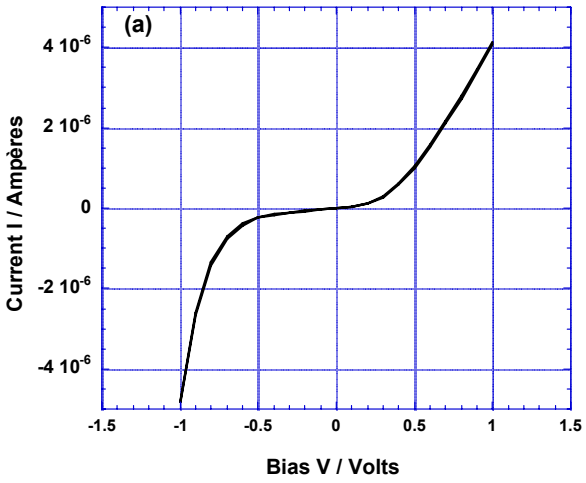

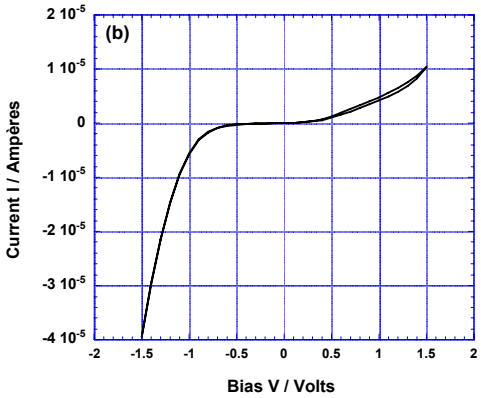

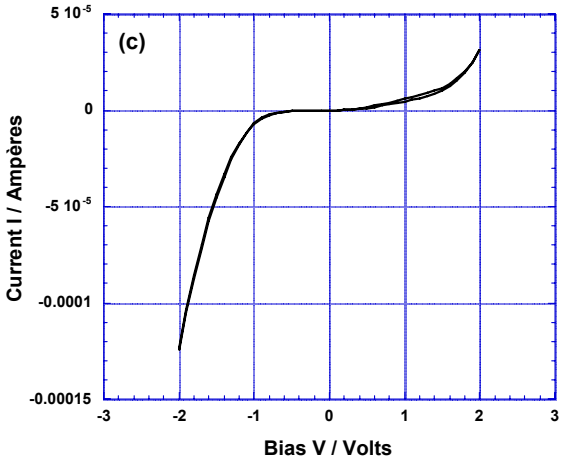

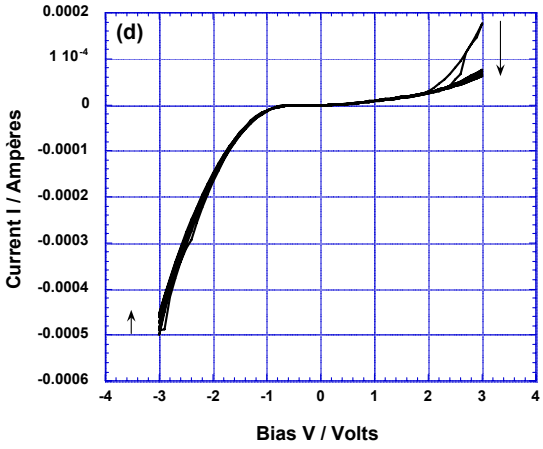

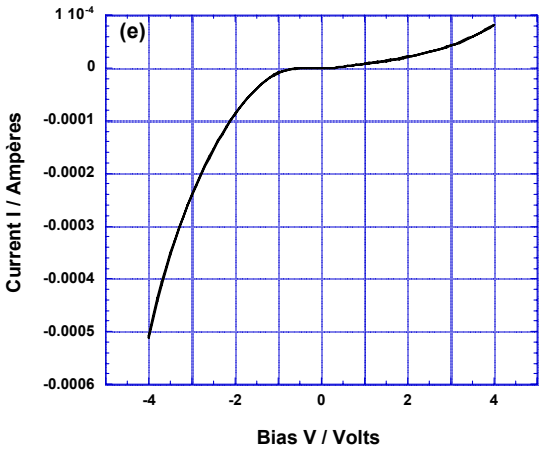

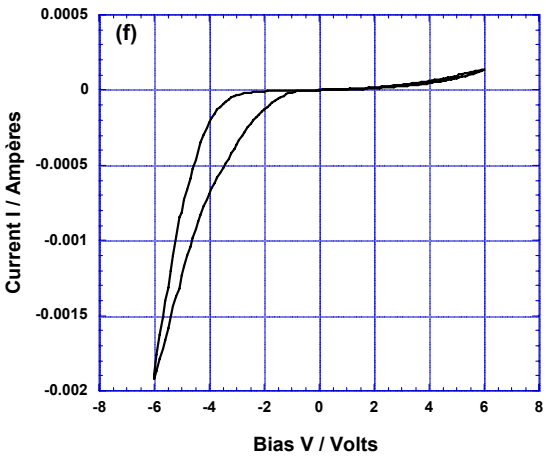

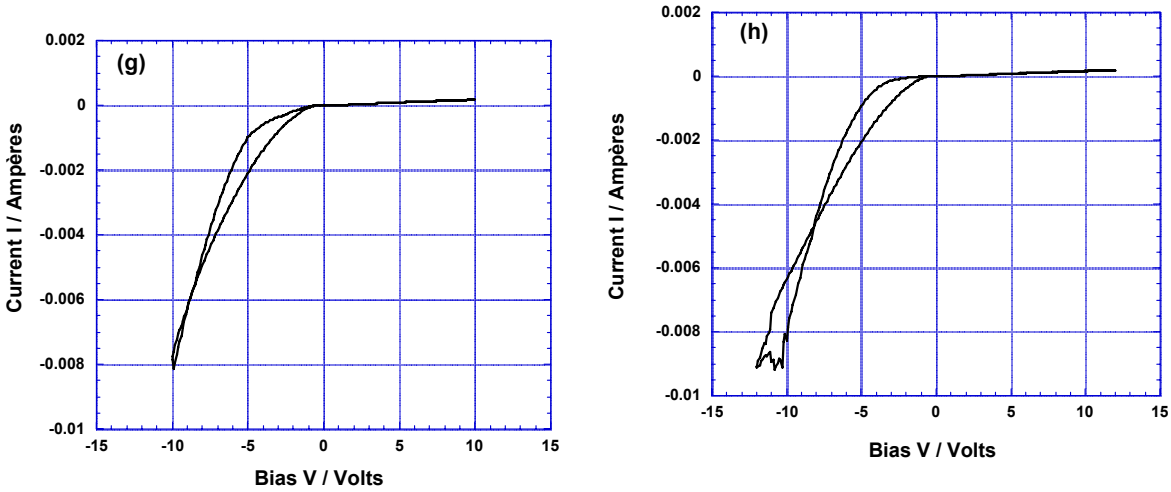

Figure Z. I-V behavior of LS monolayer of $CH_3C(O)SC_{16}H_{32}Q^+$-3CNQ$^-$, **4** sandwiched between two Au electrodes. (a) RR = 1.16 at –1 Volt; (b) RR=3.83 at – 1.5 Volts; (c) RR=3.99 at –2 Volts; (d) RR= 2.75 at – 3.0 Volts; (e) R-6.18 at – 4.0 Volts; (f) RR= 13.5 at –6.0 Volts; (g) RR= 46.1 at –10.0 Volts; (h) RR= 47.6 at –12.0 Volts (**Figure Zh** is the same as **Figure 11**)

.